Optics and Lasers in Engineering 99 (2017) 23–30

Contents lists available at ScienceDirect

Optics and Lasers in Engineering

journal homepage: www.elsevier.com/locate/optlaseng

3D model assisted fully automated scanning laser Doppler vibrometer measurements

Seppe Sels*, Bart Ribbens, Boris Bogaerts, Jeroen Peeters, Steve Vanlanduit

Op3Mech Research Group, University of Antwerp, Groenenborgerlaan 171, 2020 Antwerp, Belgium

ARTICLE INFO

Keywords:
Pose estimation
Time-of-flight
3D camera
CAD model
Scanning laser Doppler vibrometer

ABSTRACT

In this paper, a new fully automated scanning laser Doppler vibrometer (LDV) measurement technique is presented. In contrast to existing scanning LDV techniques which use a 2D camera for the manual selection of sample points, we use a 3D Time-of-Flight camera in combination with a CAD file of the test object to automatically obtain measurements at pre-defined locations. The proposed procedure allows users to test prototypes in a shorter time because physical measurement locations are determined without user interaction. Another benefit from this methodology is that it incorporates automatic mapping between a CAD model and the vibration measurements. This mapping can be used to visualize measurements directly on a 3D CAD model. The proposed method is illustrated with vibration measurements of an unmanned aerial vehicle

1. Introduction

The increasing availability of low cost and industrial 3D cameras has increased the research on 3D object recognition and pose estimation. Today object recognition and pose estimation techniques are mainly used in robotics and 3D scanning techniques. In this paper 3D measurements and processing techniques are combined with an optical vibration measurement system: the scanning laser Doppler vibrometer (SLDV).

The laser Doppler vibrometer is frequently used in the design and testing of products and structures (e.g. automotive, machine or aircraft components) [1–4]. The scanning laser Doppler vibrometer (SLDV) is an accurate instrument based on laser interferometry that can measure high spatial resolution vibration data by sequentially positioning the measurement laser beam at discrete positions using two scanning mirrors (for the vertical and horizontal deflection of the beam). Commercial SLDV's also have an integrated 2D RGB camera in which the position of the laser can be detected.

Although the SLDV is an accurate vibration measurement instrument, the measurement procedure involves a lot of user interaction: the user has to manually draw a grid of measurement locations on a 2D camera image of the measurement scene. Furthermore, the user also has to perform a calibration between the 2D image of the test object and the two laser mirror angles to aim the laser beam to the object. This can be a time consuming and tedious task that has to be repeated every time that the instrument or the test object is moved. Moreover, the manual interaction can lead to uncertainties between different measurements on the same object [5].

Our proposed methodology uses an automated calibration procedure and a 3D Time-of-Flight camera to measure the location and orientation of the test-object. The 3D image of the Time-of-Flight camera is then matched with the 3D CAD-model of the object in which measurement locations are predefined.

Currently, 3D matching techniques exist and are implemented in open source libraries like PCL-C++ libraries [6]. In our work we mainly use viewpoint feature histograms [7] to detect an object in a point cloud and for finding an initial pose estimation. An implementation of the iterative closest point algorithm is used to refine the pose estimation [8,9]. The pose estimation procedure will be elaborated in the Section 3.3.

2. State of the art

2.1. SLDV systems

Fig. 1 is a picture of the Polytec psv 300 SLDV. The SLDV has 2 movable mirrors used to aim the laser beam and a RGB camera used to see the test object and laserspot. Currently the SLDV measurement procedure requires a lot of user input. When vibration shapes of an object are measured with a traditional system the user needs to go through the following steps:

1. *Calibration* of the scanning system: in the calibration step the transformation between the image coordinates (x,y) and laser

* Corresponding author.
E-mail address: Seppe.Sels@uantwerpen.be (S. Sels).

http://dx.doi.org/10.1016/j.optlaseng.2016.09.007
Received 12 May 2016; Received in revised form 9 September 2016; Accepted 12 September 2016
Available online 23 September 2016

Fig. 1. Standard scanning laser Doppler vibrometer (Polytec psv 300).

scanning angles (θ_{hor}, θ_{ver}) are determined. To do this the user points the laser at minimum three positions on the structure and manually identifies these positions [5,10]. (see Fig. 2a).

2. *Definition of grid points* on the object in the camera-image. In commercial software, polygon drawing tools are used for this purpose (see Fig. 2b).
3. *Measure* the selected grid points (with specified frequency range, sample rate, etc.) by scanning over the defined grid points by aiming the laser beam. Fig. 2c shows an example of the output of the measurements.

During these steps, aiming the laser on a location on a structure is done by changing the angle of two integrated scanning mirrors. In order to be able to point at arbitrary locations on the structure during the measurement a mapping between the position of the laser spot and the angles of the mirrors is needed. This mapping is calculated with a 2D calibration procedure.

When the measurements are ready, they need to be interpreted and/or validated. With the traditional scanning laser Doppler vibrometer, measurements are only visualized on a standard 2D image of the object (see Fig. 1c). Measurements are also difficult to compare with values from numerical simulations (e.g. finite element analysis) because no direct geometric relation between numerical and measurements nodes is available.

Currently 3D and 2D localization techniques in combination with laser Doppler vibrometry are mainly used for measurements on moving objects. 2D techniques are used to track landmarks of a moving or rotating object and automatically aim the laser beam to a landmark position [11]. Although these methods are fast, the land-mark (white spot, reflective sticker) still needs to be applied manually. With these techniques 3D movements of the target where the landmark is distorted or only partially visible can cause inaccurate results. 3D techniques like photogrammetry are also used to track objects and aim the laser beam [12]. For accurate tracking manually applied or selected landmarks are still needed. None of the methods reported in literature provides a system that can automatically match measurements on a CAD-model and none of them can automatically select (visible) measurement points.

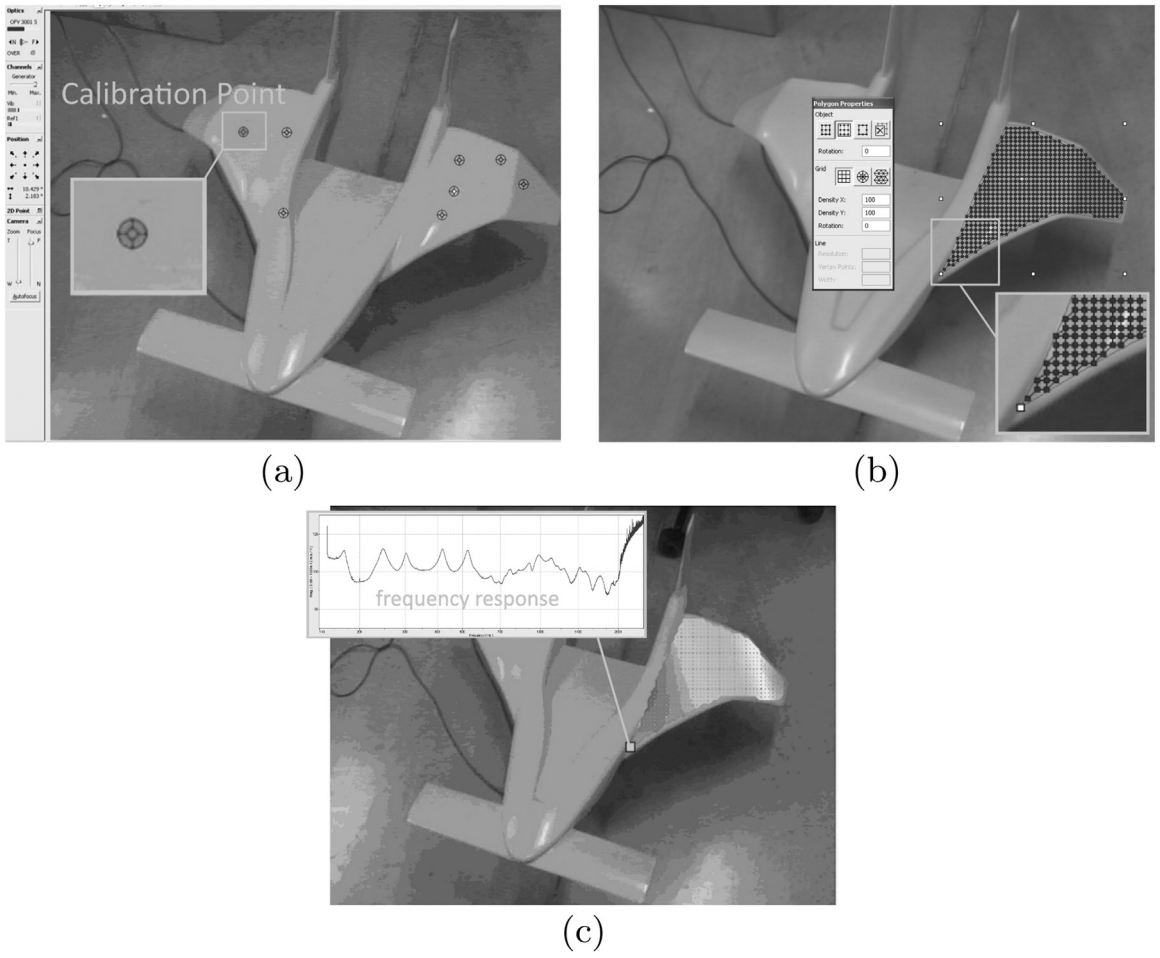

Fig. 2. (a) Manual selection of calibration points. The 8 targets on the structure show the locations where the laser spot was placed and where the user clicked. (b) Manual selection of grid points superimposed on an RGB camera image in the Polytec scanning LDV system using a polygon selection tool. (c) Graphical representation of the second operating deflection shape measured at the selected grid points and a frequency response at a selected grid point.

2.2. 3D image processing techniques

As previously stated many 3D image (3D point cloud) processing techniques are implemented in open source libraries like PCL-C++ libraries [6]. In this work two main concepts are used:

1. *Object recognition*: Which part of the 3D image is the object that is going to be measured?
2. *Object pose estimation*: How do I need to rotate and translate the CAD file to represent the real world?

Object detection techniques like Viewpoint Feature Histograms (VFH) are used to select parts of the 3D image that represents an object. With VFH-object detection a 3D point cloud (3D image) generated by the 3D camera is segmented into different clusters. Each of these clusters is described by an histogram [7]. This histogram describes (features) an object and also has bins which describe the camera position (viewpoint). The VFH's are global features because they describe all points of a point cloud (cluster) in one histogram. The histograms of the clusters are compared with histograms from a synthetic training set. This set is generated with a virtual camera at different positions and the CAD model of the sample object. The cluster with the highest similarity to a certain synthetic point cloud in the training set will be the cluster which contains points from the sample object.

Object pose estimation techniques like Fast Point Feature Histograms (FPFHs) [13] calculate the transformation between two point clouds. The FPFHs are called local features because they describe only one point in a point cloud. The FPFHs are invariant to transformations and therefore can be used to find similar points in point clouds which are translated and/or rotated compared to each other. Each FPFH of a point is matched with the corresponding FPFH of a point in the other point cloud. When point–point correspondences are known, the transformation between the two point clouds can be calculated.

3. Proposed SLDV method

3.1. Method summary

The proposed SLDV method uses an automated calibration procedure and automatically selects measurements points with the aid of a 3D CAD file and 3D Time-of-Flight camera. In addition a 2D RGB camera is used for detecting the laser spot since Time-of-Flight cameras operate in the near infra-red spectrum and therefore can not see a red laser spot. For example the laser spot of the Polytec PSV 300 system has a wavelength of 632 nm which is not visible in an near infrared (850 nm) Time-of-Flight image.

The use of the CAD model allows for a more efficient measurement process. When for example a simulation of the vibrations needs to be correlated to experimental data, nodes or critical measurement points of this simulation can be measured directly without selecting and measuring an entire grid around them. Consequently the measurement points can be stored prior the measurement-setup. During the setup the system only needs to check which points are visible and measurable. The proposed scanning methodology consists of the following steps:

1. *Step* 1: *Automatically calibrate*:
   (a) *Aim* the scanning LDV-laser at random locations (e.g. N=100) within the 2D camera-view. Aiming the laser beam is done by rotating two mirrors.
   (b) *Detect laser spot xy*-coordinates in the (RGB) image at different mirror-angles with the use of background substraction.
   (c) *Calculate mapping* between $(x, y)_{rgb}$ coordinates of the RGB-camera and scanning mirror angles $(\theta_{hor}, \theta_{ver})$. Where (θ_{hor}) defines the angle of the horizontal mirror and (θ_{ver}) the vertical mirror (the vertical mirror is visible in Fig. 4) (see Section 3.2).
2. *Step* 2: *Select visible 3D sample points* (points of interest) on the CAD model and find the corresponding coordinates on the test object.
   (a) Load predefined points of interest (measurements points).
   (b) Calculate the coordinate transformation between CAD model and 3D image using pose estimation techniques (see Section 3.3).
   (c) Convert the loaded points of interest to the 3D image coordinate system.
   (d) Perform a visibility analyses to select sample points (visible point of interest).
3. *Step* 3: *Measure* the vibrations at the predefined locations of interest (see Section 3.4).

The end user only needs to provide the points of interest and needs to define LDV specific measurement settings (sample period, frequency resolution, etc.)

3.2. Step 1: Calibration

The new calibration procedure uses the 2D coordinate system of an RGB camera like the traditional techniques but is fully automatic. The calibration calculates d (distance between sample point and camera) and d_0 (space between the two mirrors of the SLDV) from Eqs. (1) and (2) with singular value decomposition. The procedure is based on work of [14]:

$$x = d\tan(\theta_{hor}) \tag{1}$$

$$y = d_0 + \frac{d\tan(\theta_{ver})}{\cos(\theta_{hor})} \tag{2}$$

The laser spot is detected by background subtraction of a reference frame F_{ref} (where no laser-spot is seen) and a frame F_{spot} where the lasers pot is visible. The highest values of this difference image ($F_{diff} = F_{spot} - F_{ref}$) will indicate the position of the laser spot. When the highest value is below a threshold, the laser is repositioned because it is not visible in the 2D image.

3.3. Step 2: Select visible 3D sample points

To accurately aim the SLDV, the 3D position of the sample-object is needed. This position is calculated in the 3D camera coordinate system with a 3D pose calculation technique. The proposed pose calculation technique is built on work of [6,7,13,15]. The 3D pose calculation can be divided in two main parts:

1. *Object detection*: In this step measured 3D points that describes the sample object are searched. This step is summarized as 'global' pipeline in Fig. 3. The global pipeline searches for clusters (segments) that belong to the object and finds a first approximately view of the point cloud by comparing the clusters with a training set with the aid of Viewpoint Feature Histograms (VFH).
2. *Object pose estimation*: In this part the transformation $T_{cad\rightarrow 3D}$ between the CAD model and the measured point cloud is calculated. This step is summarized as 'local' pipeline in Fig. 3. The local pipeline uses local point features to describe points in both the captured cluster and the synthetic view from the training set. After matching of these features, the iterative closest point algorithm (ICP) is used to refine the results. ICP refines the results by minimizing the distance between the measured point cloud and the synthetic point cloud (where the synthetic point cloud is transformed with the previously found pose estimation)

The result of the pose estimation is the transformation $T_{synt\rightarrow clust}$ between the synthetic point cloud (CAD model) and the measured

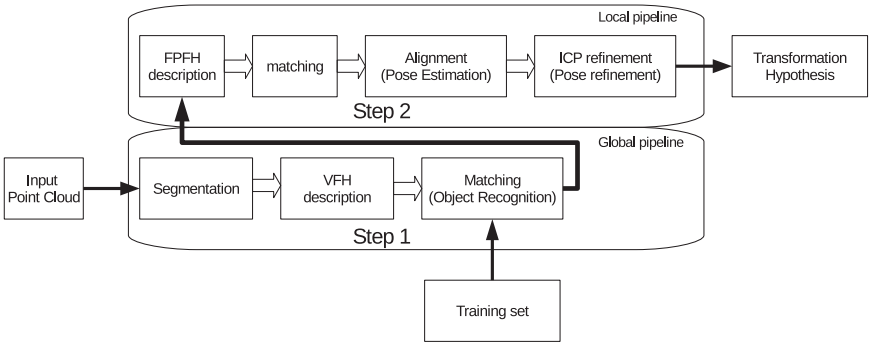

Fig. 3. Object transformation pipeline. The pipeline is divided in a global and a local pipeline.

point cloud.

In the next phase visible points of interest are selected on the measured point cloud. These points of interest can be predefined in the CAD model, or they can be obtained from a mesh from e.g. numeric simulations of the vibration shape. Using a mesh from numeric simulations provides a direct mapping between measured points and simulated points. To find visible points of interest (sample points) a visibility analysis in combination with the calculated object-transformation is used to select visible sample points.

3.4. Step 3: Measurements

After step 1 (Calibration) and step 2 (Pose calculations), the 3D position of the visible sample points will be converted to the 2D coordinate system of the RGB camera. Next these 2D coordinates will be converted to the corresponding mirror angles of the SLDV (see Eqs. (1) and (2)). After aiming the laser with these mirror angles, the selected points of interest will be measured by the SLDV. Note that the procedure does not automatically select LDV specific settings like sample period, frequency range, etc..

4. Experimental setup

A Kinect for Xbox One (Kinect One) is used for measuring 3D images. This device consists of a 3D Time-of-Flight (ToF) camera and a 2D RGB camera. The Kinect for Windows SDK provides a pre-calibrated mapping between the 2D RGB coordinate system and the 3D ToF system. The 3D ToF sensor is used for 3D measurements of the object at frame rates up to 30 frames/second. The measurements will be in the form of a 3D point cloud (see Fig. 8). Since the ToF sensor is an infrared sensor equipped with a band pass near infrared filter, the laser spot is not visible in the 3D image. The integrated 2D RGB camera is used in the calibration procedure (Section 3.2) for detecting the laser spot. The Kinect One is mounted below a scanning laser Doppler vibrometer (Polytec type PSV 300) (see Fig. 4). As test-object a model of a unmanned aerial vehicle that was developed by the company Nimbus for the Seventh Framework Program EU project Acheon[1] is used. The size of the wings of the model from wing-tip to wing-tip is 80 cm

5. Results and discussion

5.1. Procedure

With our methodology it is possible to correlate the LDV measurements directly with the CAD model. As a result it is easier to compare real measurements with numerical simulations. In Fig. 5 we compare the result of a traditional scanning method (using Polytec software) with the result of the proposed procedure. The measurements are mapped on a 2D view of the object. With our procedure (Fig. 5a) the scanning grid is directly mapped on the CAD file.

The standard procedure (without the actual vibration measurements) takes approximately 8 min of setup time (depends on the number of sample points selected). The proposed procedure has no manual set-up time (just place the object in front of the system). The 'automatic' setup of the procedure (calibration and sample point selection) takes approximately 2 min (see Table 1). The first advantage of the automatic set-up is that the user does not need to do a cumbersome calibration and user dependant sample-point selection. The automatic procedure also makes sample point selection more repeatable then manual selection. The main advantage of the procedure is seen after the measurements because they are available in CAD-coordinates. Each measured point and measurement direction is known in the coordinate system of the CAD-file. This allows easy comparison with numeric simulations of the vibration shapes.

5.2. Results calibration

In Fig. 6a the true (applied) angle and calculated angles are shown. Some outliers exist due to erroneously detected sample points. The rms value of the difference between true and calculated angles is 0.10° where the outliers (angles larger then 20°) are excluded from the rms-calculation.

An example of aiming the laser after the calibration procedure is shown in Fig. 6b. The error on the positioning of the laser is shown in Fig. 6c. This error is caused by the fact that the calibration procedure is a 2D procedure while we are aiming at a 3D object. In addition the separation (distance) between the two mirrors can cause a systematic error [16]. Because 3D measurements are available, the methodology could be extended to a 3D calibration procedure.

In our measurements positioning of the laser is accurate for about 4 mm. After calibrating a new set of random points (100) (located on the sample object) is defined. Then for every point the angles are calculated and the laser is aimed. After aiming, for every point the position of the spot is detected. The measured and input positions are then converted to *XYZ* coordinates (with the Kinect One 3D image). The position error is then calculated as the distance between the two sets. The mean error is equal to 3.7 mm the standard deviation 1.9 mm. The error is in the same order as the size of the laser spot in the 2D RGB image ± 10 mm. Note that this error also contains the noise of the 3D measurement. The size of the model from wing-tip to wing-tip is 80 cm.

5.3. Results pose calculation

In Fig. 7a the measured point cloud is clustered into different clusters. Each cluster VFH is compared with the VFH of the synthetic pointclouds generated by a virtual camera (see Fig. 7b). After the object is detected, the transformation between the simulated pointcloud with

[1] http://acheon.eu/nimbus-develops-innovative-uav-configuration-for-the-acheon-experiments/ for more information.

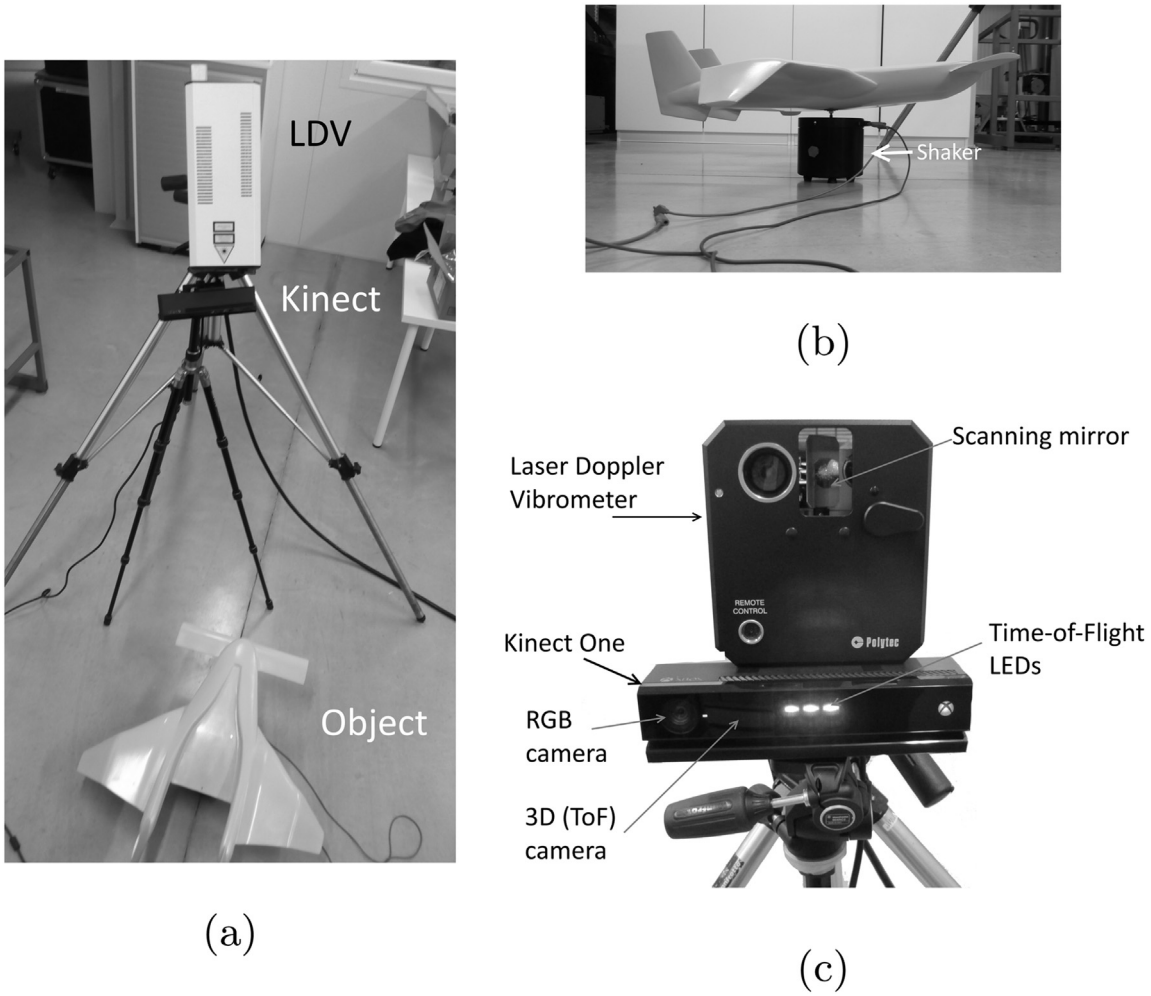

Fig. 4. (a) Experimental setup. Kinect One 3D camera mounted below a Polytec PSV 300 scanning LDV aimed at the sample-object.(b) Sample object mounted on a electromagnetic shaker. (c) Kinect One 3D camera and front of scanning LDV.

the highest similarity (see Fig. 8) and the measured pointcloud is calculated with FPFH matching and ICP. After this matching the transformation between the CAD model and the measured point cloud is known (see Fig. 8). Next a visibility analysis is performed and visible sample points are selected. In Fig. 8 the visible points (only the top) of the wing are selected.

5.4. Discussion pose calculation

In our experiments, the mean euclidean distance between the measured point cloud and the transformed CAD model 2 mm. This error indicates that the mean position error of the measurement points is 2 mm.

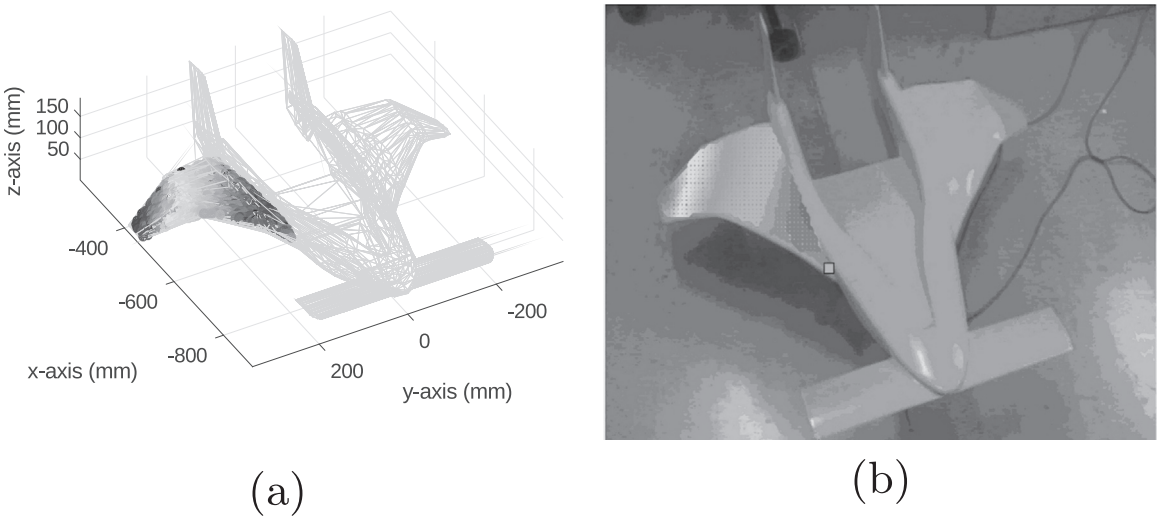

Fig. 5. Comparison between (a) our new 3D method and (b) the original output from Polytec.

Table 1
Comparison between the proposed and traditional procedure. The sample point selection in the traditional procedure is highly user dependant and takes longer with more complex shapes.

Steps	Traditional procedure (min)	Proposed procedure (min)
Step 1: Calibration	3	1
Step 2: Sample point selection	5	1

The two different stages (global and local) of the pose estimation combines the power of viewpoint feature histograms (global) and fast point feature histograms (local). Viewpoint feature histograms are very good for object recognition but since they are camera roll independent they can give wrong pose estimations. Fast point feature histograms are good at finding the transformation between two similar point clouds [17]. Therefore, we compare the FPFHs from the cluster with the features of the similar synthetic view obtained from the VFH-matching. In [18] a similar approach is investigated and an average accuracy (correct object and pose recognition) of 89% is stated. Where our approach is different in the fact that the measured object is known where the algorithm of [18] can choose between multiple objects. Note that there are other techniques available like CVFH (clustered VFH), OUR-CVFH (Oriented, Unique and Repeatable CVFH), camera-roll histogram, Hough-voting, that use only global features to find a pose estimation [19–21]. Most of these algorithms are derived from feature matching techniques (like FPFH). Because of the good documentation and reliability of FPFH pose estimation this technique is used in combination with the global pipeline (used for object detection). In some cases other techniques might improve the pose estimation. For instance the technique used in this methodology will fail if sample objects are occluded by other objects.

6. Conclusion

Current techniques require a lot of user interaction during the calibration of the SLDV-system and setup of the measurement. Our methodology eliminates this user interaction with an automated calibration procedure and the detection of the sample-object using a the 3D model of the object and a 3D camera. The methodology also incorporates automatic mapping between a CAD model and the vibration measurements. This mapping is used to directly visualize measurements on a 3D CAD model. This mapping also can be used to directly correlate measurements and numeric simulations because

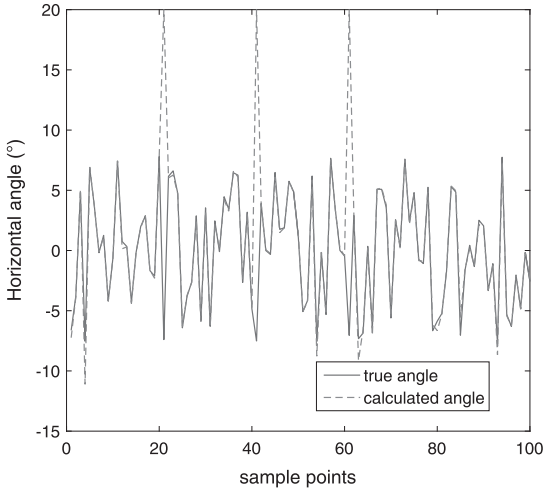

(a)

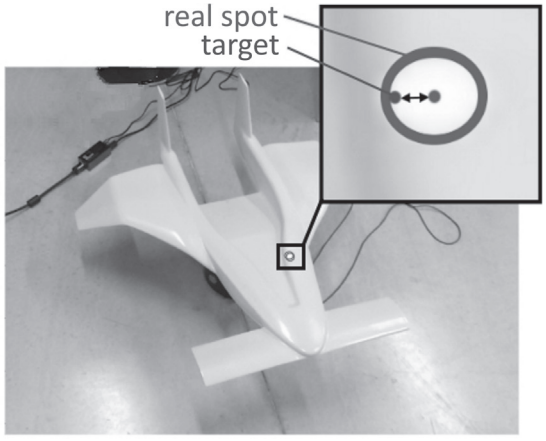

(b)

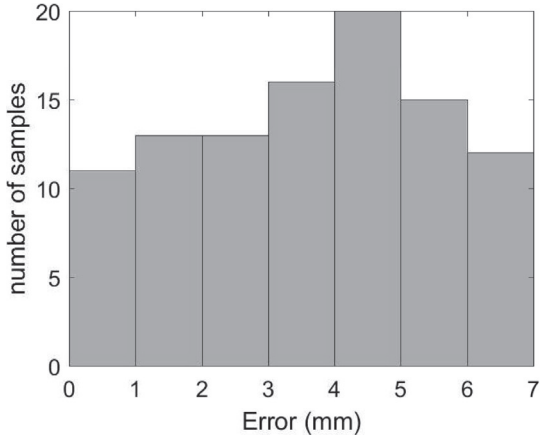

(c)

Fig. 6. (a) Comparison between true (applied) angle and calculated angles (only horizontal angles are shown). (b) Example image with detected laser spot and target laser spot. The distance between the two points is 4 mm and the diameter of the laser spot is 10 mm. (c) Histogram of the positioning error of the laser spot for 100 validation points. The distance between (new) target coordinates and coordinates of the aimed laser spot is shown.

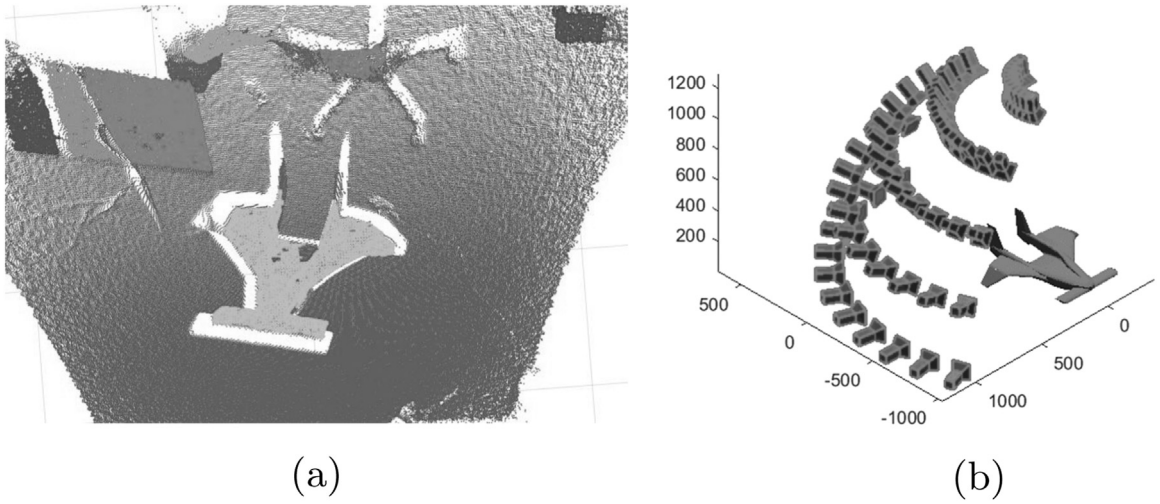

Fig. 7. (a) Example of a (segmented) point cloud. Different detected clusters are visualized in different colors/grayscale. (b) Partial (1/4) set of training-views. Virtual cameras are located in a sphere around the CAD model. (For interpretation of the references to color in this figure caption, the reader is referred to the web version of this paper.)

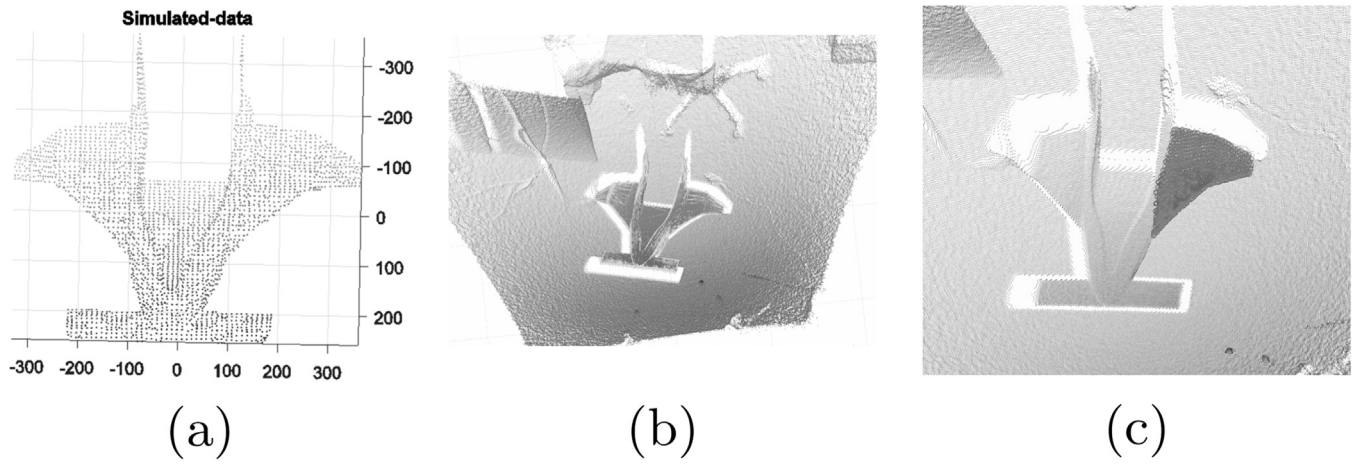

Fig. 8. (a) Example of a simulated point cloud. (b) Example of the matched CAD model (yellow,lines) and a measured 3D point cloud (blue, points). (c) Example of visible sample points (red/dark) of the left wing plotted on top of the measured point cloud. (For interpretation of the references to color in this figure caption, the reader is referred to the web version of this paper.)

measurements are directly available in the CAD-coordinate system. The location of each measurement in the CAD coordinate system is accurate up to ± 4 mm. The correlation also needs to take in account that although the 1D LDV vibration measurements are available in a 3D CAD system, measurements are still in one direction.

References

[1] Pickering C, Halliwell N, Wilmshurst T. The laser vibrometer: a portable instrument. J Sound Vib 1986;107(3):471–85. http://dx.doi.org/10.1016/S0022-460X(86)80119-5.
[2] Sitnik L, Pentoś K, Magdziak-Tokłowicz M, Wrobel R. The laser Doppler vibrometry in mechatronics diagnostics. Arch Civil Mech Eng 2015;15(4):962–70. http://dx.doi.org/10.1016/j.acme.2015.04.001.
[3] Katunin A, Dragan K, Dziendzikowski M. Damage identification in aircraft composite structures: a case study using various non-destructive testing techniques. Compos Struct 2015;127:1–9. http://dx.doi.org/10.1016/j.compstruct.2015.02.080.
[4] Halkon BJ, Rothberg SJ. Angular (pitch and yaw) vibration measurements directly from rotors using laser vibrometry. Mech Syst Signal Process 2014;46(2):344–60. http://dx.doi.org/10.1016/j.ymssp.2014.01.013.
[5] Martarelli M, Revel G, Santolini C. automated modal analysis by scanning laser vibrometry: problems and uncertainties associated with the scanning system calibration. Mech Syst Signal Process 2001;15(3):581–601. http://dx.doi.org/10.1006/mssp.2000.1336.
[6] Rusu RB, Cousins S. 3D is here: point cloud library. In: IEEE international conference on robotics and automation; 2011. p. 1–4. http://dx.doi.org/10.1109/ICRA.2011.5980567 URL ⟨http://pointclouds.org/⟩
[7] Rusu RB, Bradski G, Thibaux R, Hsu J. Fast 3D recognition and pose using the viewpoint feature histogram. In: IEEE/RSJ 2010 international conference on Intelligent Robots and Systems, IROS 2010 – Conference Proceedings; IEEE; 2010. p. 2155–62. http://dx.doi.org/10.1109/IROS.2010.5651280.
[8] Bergström P. Computational methods for on-line shape inspection [Ph.D. thesis]. Luleå University of Technology; 2009.
[9] Bellekens B, Spruyt V, Weyn M. A Survey of rigid 3D pointcloud registration algorithms. In: AMBIENT 2014, the fourth international conference on ambient computing, applications, services and technologies 2014; 2014. p. 8–13.
[10] GmbH P. Polytec scanning vibrometer 8.7 software manual 2004.
[11] Castellini P. Vibration measurements by tracking laser Doppler vibrometer on automotive components. Shock Vib 2002;9(1–2):67–89.
[12] Jennings A, Black J, Allen C, Simpkins J, Sollars R. Vibrometer steering system for dynamic in-flight tracking and measurement. Exp Mech 2011;51(1):71–84. http://dx.doi.org/10.1007/s11340-010-9337-3.
[13] Rusu RB, Blodow N, Beetz M. Fast Point Feature Histograms (FPFH) for 3D registration. In: 2009 IEEE international conference on robotics and automation; 2009. p. 3212–7. http://dx.doi.org/10.1109/ROBOT.2009.5152473.
[14] Vanlanduit S, Guillaume P, Cauberghe B, Verboven P. An automatic position calibration method for the scanning laser Doppler vibrometer. Meas Sci Technol 2003;14(8):1469–76. http://dx.doi.org/10.1088/0957-0233/14/8/336.
[15] Rusu RB, Marton ZC, Blodow N, Beetz M, Persistent point feature histograms for 3D point clouds. 2008. http://dx.doi.org/10.3233/978-1-58603-887-8-119.
[16] Halkon BJ, Rothberg SJ. Vibration measurements using continuous scanning laser Doppler vibrometry: theoretical velocity sensitivity analysis with applications. Meas Sci Technol 2003;14(3):382.
[17] Hänsch R, Weber T, Hellwich O. Comparison of 3D interest point detectors and descriptors for point cloud fusion. ISPRS Ann Photogramm Rem Sens Spatial Inf Sci 2014;II-3(September):57–64. http://dx.doi.org/10.5194/isprsannals-II-3-57-2014.
[18] Alhamz K, Elmogy M, Barakat S. 3D object recognition based on local and global features using point cloud library. Int J Adv Comput Technol (IJACT). 2015;7(3).

[19] Aldoma A, Tombari F, Rusu RB, Vincze M. OUR-CVFH – oriented, unique and repeatable clustered viewpoint feature histogram for object recognition and 6DOF pose estimation. In: Lecture notes in computer science – LNCS (including subseries lecture notes in artificial intelligence and lecture notes in bioinformatics), vol. 7476; 2012. p. 113–22. http://dx.doi.org/10.1007/978-3-642-32717-9_12.

[20] Aldoma A, Tombari F, Stefano LD, Vincze M. A global hypotheses verification method for 3D object recognition. In: Eccv; 2012. p. 511–24. http://dx.doi.org/10.1007/978-3-642-33712-3_37.

[21] Tombari F, Stefano LD. Hough voting for 3D object recognition under occlusion and clutter. IPSJ Trans Comput Vis Appl 4;2012:20–9. http://dx.doi.org/10.2197/ipsjtcva.4.20.